Published in final edited form as:

JACC Clin Electrophysiol. 2018 December ; 4(12): 1501–1515. doi:10.1016/j.jacep.2018.08.024.

Human Atrial Fibrillation Drivers Resolved with Integrated Functional and Structural Imaging to Benefit Clinical Mapping

Brian J. Hansen, BSc[a,b], **Jichao Zhao, PhD**[c], **Ning Li, MD, PhD**[a,b], **Alexander Zolotarev, BSc**[a,d], **Stanislav Zakharkin, PhD**[a], **Yufeng Wang, BSc**[c], **Josh Atwal**[c], **Anuradha Kalyanasundaram, PhD**[a,b], **Suhaib H. Abudulwahed**[a], **Katelynn M. Helfrich, BSc**[a], **Anna Bratasz, PhD**[b], **Kimerly A. Powell, PhD**[b], **Bryan Whitson, MD**[b,e], **Peter J. Mohler, PhD**[b,f], **Paul ML. Janssen, PhD**[a,b], **Orlando P. Simonetti, PhD**[b,g], **John D. Hummel, MD**[b,f], and **Vadim V. Fedorov, PhD**[a,b]

[a]Department of Physiology & Cell Biology, The Ohio State University Wexner Medical Center, Columbus, OH, USA. [b]Davis Heart & Lung Research Institute, The Ohio State University Wexner Medical Center, Columbus, OH, USA. [c]Auckland Bioengineering Institute, The University of Auckland, Auckland, New Zealand [d]Moscow Institute of Physic and Technology, Dolgoprudny, Russian Federation [e]Department of Surgery, The Ohio State University Wexner Medical Center, Columbus, OH, USA. [f]Department of Internal Medicine, The Ohio State University Wexner Medical Center, Columbus, OH, USA. [g]Department of Biomedical Engineering, The Ohio State University Wexner Medical Center, Columbus, OH, USA.

Abstract

Background: Clinical multi-electrode mapping of atrial fibrillation (AF) drivers suffers from variable contact, signal processing, and structural complexity within the 3D human atrial wall, raising questions on the validity of such drivers.

Objectives: To improve AF driver identification by integrating clinical multi-electrode mapping with driver fingerprints defined by high-resolution ex-vivo 3D functional and structural imaging.

Methods: Sustained AF was mapped in coronary-perfused explanted human hearts (n=11) with transmural near-infrared optical mapping (NIOM, ~0.3mm^2 resolution). Simultaneously, custom FIRMap catheters (~9×9mm^2 resolution) mapped endocardial and epicardial surfaces, which were analyzed by Focal Impulse and Rotor Mapping (FIRM) activation and Rotational Activity Profile (RAP). Functional maps were integrated with contrast-enhanced MRI (CE-MRI, ~0.1mm^3 resolution) analysis of 3D fibrosis architecture.

Results: During sustained AF, NIOM identified 1-2 intramural, spatially stable reentrant AF drivers per heart. Driver targeted ablation affecting 2.2±1.1% of the atrial surface terminated and

Address for correspondence: Vadim V. Fedorov, PhD, Department of Physiology and Cell Biology, The Ohio State University Wexner Medical Center, 5196 Graves Hall, 333 W 10th Ave, Columbus OH 43210-1218, tel: 1-614-366-0986; fax: 1-614-292-4888, vadim.fedorov@osumc.edu.

prevented AF. Driver regions had significantly higher phase singularity density, and dominant frequency versus neighboring non-driver regions. FIRM had 80% sensitivity to NIOM-defined driver locations (16/20), and matched 14/20 driver visualizations: 10/14 reentries seen with RAP, and 4/6 breakthrough/focal patterns. FIRM detected 1.1±0.9 false-positive RAP per recording, but these regions had lower intramural CE-MRI fibrosis than driver regions (14.9±7.9% vs 23.2±10.5%, $p<0.005$).

Conclusion: The study revealed that both reentrant and breakthrough/focal AF driver patterns visualized by surface-only clinical multi-electrodes can represent projections of 3D intramural microanatomic reentries. Integration of multi-electrode mapping and 3D fibrosis analysis may enhance AF driver detection, thereby improving the efficacy of driver targeted ablation.

Condensed Abstract

Clinical multi-electrode mapping has limited ability to localize atrial fibrillation (AF) drivers. To validate clinical mapping, intramural reentrant AF drivers were defined in ex-vivo human atria by high-resolution transmural optical mapping and 3D contrast-enhanced MRI (CE-MRI). Simultaneous clinical multi-electrode mapping visualized 3D reentrant AF drivers with 80% sensitivity as reentrant and breakthrough/focal surface patterns. False-positive rotation patterns visualized by clinical multi-electrode mapping could be distinguished from AF drivers by CE-MRI intramural fibrosis analysis, suggesting the efficacy of targeted ablation could be improved by integrating multi-electrode mapping and 3D fibrosis analysis.

Keywords

Atrial Fibrillation; Drivers; Optical Mapping; Multi-electrode Mapping; Contrast-enhanced MRI; Fibrosis

Introduction

Atrial fibrillation (AF) affects over 33 million people worldwide and is a leading cause of hospitalization and mortality.(1,2) Recent evidence from experimental and clinical studies suggests that AF may be maintained by localized AF drivers, which are finite regions of fast, repetitive conduction in both left and right atria (RA).(3-5) Targeted ablation of AF drivers guided by panoramic multi-electrode mapping techniques, such as Focal Impulse and Rotor Mapping (FIRM) and Electrocardiographic Imaging (ECGI), is used at healthcare centers worldwide with considerable success rates in AF treatment.(5,6) However, some studies using the same techniques have reported much lower success rates.(6,7) Furthermore, recent high density local multi-electrode mapping during open-chest procedures did not visualize any AF drivers.(8) Therefore, resolving controversies in identifying as well as clarifying the role of drivers in human AF is of utmost importance to the field of AF ablation.(9)

The complex 3D structure of human atria(10,11) remains a critical obstacle in identifying AF drivers for all clinical electrode mapping approaches, which are limited to endocardial/epicardial surface-only recordings. Moreover, unvalidated analysis of fractionated clinical electrograms may incompletely represent or miss intramural AF drivers.(12) Nonetheless, some of these electrogram limitations could be mitigated by phase mapping, which bypasses

the need for annotating local activation times(13) and has been utilized in clinical mapping, such as ECGI(4) and FIRM, to highlight rotation by phase singularities (PS) and Rotational Activity Profiles (RAP).(13) However, phase processing can create false-positive artificial "drivers", which obscure AF driver detection in clinical settings.(11,14)

Therefore, the accuracy of clinical mapping may be reliably determined from direct validation of transmural conduction within the complex 3D human atria. Our recent studies have revealed that dual-sided high-resolution near-infrared optical mapping (NIOM) of the explanted, coronary-perfused human atria, integrated with high-resolution 3D contrast-enhanced MRI (CE-MRI), can "interpolate" conduction patterns of intramural reentrant AF drivers that appear as breakthrough or focal patterns projected onto endocardial or epicardial surfaces.(15-17)

Hence, the goals of this ex-vivo human atrial study are to (1) simultaneously map ex-vivo human atria with the clinically-used electrode mapping system, FIRM, and dual-sided transmural NIOM, to assess if reentrant or breakthrough/focal activation patterns in human AF, seen clinically, represent AF drivers; (2) identify unique patterns or "fingerprints" of AF driver regions by integrating functional and structural features from NIOM and multi-electrode mapping with 3D CE-MRI analyses to distinguish true-positive AF drivers from false-positive "drivers".

Methods

An expanded Methods section can be found in the Online Appendix.

Explanted Human Hearts and Inclusion Criteria

De-identified, coded human hearts were obtained from The Ohio State University Cardiac Transplant team and LifeLine of Ohio in accordance with The Ohio State University Institutional Review Board. Patient-specific data can be found in Online Table 1 and the procedures performed on each atrial preparation and the type of preparation are listed in Online Table 2. Only atrial preparations with sustained AF (>1min) induced by burst pacing and localized drivers confirmed by NIOM were included in this study's driver analysis (n=11). The current study presents entirely new analyses and techniques, such as integrated phase singularity density, multi-electrode mapping, and 3D CE-MRI fibrosis analysis.

Near-Infrared Optical Mapping of Coronary-Perfused Human Atria to Define AF Driver Regions Human intact biatrial (n=2), RA (n=8), and left atrial (LA) (n=1) preparations were isolated, coronary-perfused, immobilized, and stained, as previously described (Online Figure 1).(15,16) Biatrial or dual-sided NIOM was conducted during sustained AF and data were analyzed to identify AF drivers by dV/dt_{max} activation mapping and dominant frequency (DF) analysis.(15,16) Driver activation patterns were classified as reentrant or breakthrough, both patterns were shown by dual-sided NIOM to be caused by intramural reentry (Online Figure 2).(16) Online Table 3 lists the conditions under which sustained AF was induced, number of drivers, and driver visualization pattern for each AF episode. Hilbert Transform of optical action potentials (OAPs) was used to calculate the local phase(18), PS,

and PS density (PSD), which was calculated for each pixel as the percentage of total temporal frames (Figure 1B).

Termination of AF to normal sinus rhythm or atrial tachycardia by targeted radiofrequency ablation applied endocardially to reentrant tracks (Online Figure 3) was used to confirm NIOM-defined AF drivers as the mechanism of sustained AF.(15) The endocardial surface area for targeted ablation (that which terminated AF, converted to atrial tachycardia, or slowed AF by ≥10%), untargeted ablation (a negative control which was outside the driver region and had no effect on driver dynamics or global AF pattern), and ablation of atrial tachycardia was calculated relative to total endocardial surface area.

Integration of Focal Impulse and Rotor Mapping

To compare NIOM and clinical multi-electrode mapping, two 64-electrode (8×8) FIRMap catheters (Abbott Labs, Chicago, IL) with the standard resolution of ~9×9mm^2 were customized and flattened so they could map both epicardial and endocardial lateral atrial surfaces. The flattened FIRMap catheter has the same electrode size and inter-electrode distances as its clinical counterpart (Online Figure 1). RhythmView 6.1 (Abbott Labs, Chicago, IL) processed AF activation patterns. Blinded to NIOM and structural data, unipolar activation times for a 4s FIRM epoch within NIOM recordings were marked manually by Abbott engineers in accordance with the RhythmView criteria. RAP marked by RhythmView 6.1, which combines unipolar electrogram derived PSD and activation maps, was used to define reentrant patterns of AF drivers by FIRM.(13) Focal patterns were defined as activation beginning at one or more electrodes simultaneously and spreading outward. The location of a driver was congruent between NIOM and FIRM if the location differed by ≤1 inter-electrode distance. RAP locations not matched with a NIOM-defined AF driver were considered false-positives. For electrogram DF analysis, each unipolar atrial electrogram from the catheter was filtered using a Butterworth filter, and then DF was estimated using a Fast Fourier Transform.

Contrast-Enhanced Magnetic Resonance Imaging

Gadolinium-based CE-MRI (9.4 Tesla) was used to define atrial anatomy (Online Figure 1) and 3D fibrosis distribution at a resolution of 0.09-0.18mm^3, which is significantly higher than could be obtained by current clinical CE-MRI (~1.25mm^3 by 3 Tesla), allowed the sub-division of the atrial wall into sub-epicardium, intramural wall, and sub-endocardium, as previously described.(17)

CE-MRI-detected fibrosis is reported as the percent of gadolinium-enhanced voxels, based on intensity thresholds defined by comparing CE-MRI with histology, within the sub-volume of the atrial wall.

Statistical Analysis

Data are presented as mean ± standard deviation. Pairwise comparisons were done with Tukey adjustment. Analysis was done in R 3.4.1 using packages lme4 and lsmeans. Pearson correlation was used to evaluate agreement between NIOM and FIRM results. P-values ≤0.05 were considered significant.

Results

AF Driver Identification by NIOM in the Human Heart Ex-Vivo

AF driver dynamics were analyzed in 17 episodes of sustained AF in 2 intact atria, 8 isolated lateral RA, and 1 isolated LA. Thirty-four AF driver visualizations were recorded, either simultaneously from the sub-endocardium and sub-epicardium in the isolated RA/LA (n=14 × 2=28) or recorded from the sub-epicardium in the intact atria (n=6). During sustained AF, NIOM wavefront activation maps revealed 1.2±0.4 AF drivers per episode (Figure 1A). All drivers were spatially stable, but in three hearts (947200, 402879, and 728878), when two drivers were present in the same episode, the temporal stability of each could be <100%, yet AF drivers repeatedly returned to and remained at the same anatomical location.(16,17) Reentrant and breakthrough patterns were both seen in driver regions (Online Table 3). Similar to earlier findings,(15) localized intramural reentry (n=14) mapped by dual-sided NIOM was seen more often as reentry from the endocardium, and the same driver visualized from the epicardium could show a stable breakthrough pattern (n=7). Radiofrequency ablation targeting the pivot points of NIOM-defined reentrant drivers confirmed they were the sustaining mechanism in 10/10 AF episodes each lasting ≥10min (Online Figure 3 and Online Table 2). Driver targeted ablation covered 2.2±1.1% of the endocardial surface, and AF terminated or converted to atrial tachycardia 92±36s after the last targeted AF ablation application. Atrial tachycardia ablation, necessary in 4 atria, covered 1.2±1.0%, and untargeted ablation, used in 4 atria, covered 1.3±0.5%, but had no effect of AF dynamics (Online Table 2). A total of 3.5±1.4% of the endocardial surface was ablated until arrhythmia could not be induced.

Identifying AF Driver Regions by NIOM Phase Mapping

Phase processing was applied to NIOM OAPs to assess if AF drivers in the human heart could be visualized by their resulting PS distribution and density (Figure 1). Figure 1A shows an activation map of a temporally and spatially stable reentrant driver, and Figure 1B shows PSs were present primarily near the pivoting points. While PSs were intermittent and discontinuous throughout one reentry cycle, PSD mapping showed the highest density along the reentry track, formed by several partially insulated pectinate bundles seen by 3D CE-MRI. PSs could also be present outside the reentrant track due to wavebreaks, primarily at discontinuous or twisted myobundles, but occurred with a lower PSD. All AF driver regions had significantly higher average and maximum PSDs of 0.39±0.26% and 3.14±2.67% vs 0.20±0.18% ($p<0.05$) and 0.87±0.74% ($p<0.01$) for non-driver regions, respectively. However, in cases where the intramural reentrant drivers were visualized with a breakthrough pattern from either sub-endocardial or sub-epicardial NIOM, phase mapping did not have the distinguishable clusters of high PSD that were present on maps from the other atrial surface where a reentrant pattern was visualized (Figure 1C, Online Figure 2). Separating AF driver regions into their visualization patterns showed average PSD to be significantly higher only in those drivers visualized as reentrant and not breakthrough patterns (Figure 1D).

Sensitivity and False-Positive Rate of AF Driver Detection by Clinical Multi-Electrode Catheters Compared to NIOM

In 6 hearts, we estimated the correlation between FIRM and NIOM for activation patterns and AF driver visualization. Figure 2A shows that activation patterns during 500ms CL pacing were similar between the two methods, and the total activation time across the optical field of view correlated. During sustained AF, driver DF seen by FIRM and NIOM was also strongly correlated (Figure 2B, Online Table 3). Next, we compared AF driver visualization between NIOM and FIRM, which were analyzed blinded to each other (Online Table 3). Figure 3A shows an activation map of two competing reentrant drivers identified by NIOM that were characterized by clusters of high PSD. Clusters of RAP were present within or near NIOM reentry tracks (Online Movie 1). Figure 3B shows OAPs and FIRM electrograms on the reentrant driver track confirming repetitive reentrant activity. During sustained AF, FIRM identified 16/20 NIOM-defined AF driver locations within one inter-electrode distance. RhythmView visualized RAP at 10/14 reentrant AF driver regions. Additionally, 4/6 breakthrough patterns defined by NIOM were also visualized by FIRM as focal activation (Figure 4A, Online Movie 2, Right panel). Figure 4B shows one of the two instances when a reentrant driver identified by epicardial NIOM was seen as a focal activation pattern by epicardial FIRM. This observation was consistent as shown in Online Figure 4 by five consecutive activation maps for this case from both epi and endocardium seen by both NIOM and FIRM simultaneously. Online Figure 5 shows FIRM correctly identified the NIOM-defined post-ablation AF driver in the isolated LA preparation as well. Furthermore, two reentrant and two breakthrough/focal NIOM AF driver patterns were unidentified by FIRM, and seen only as chaotic activation (Online Movie 2, Left panel). In two of these cases the electrodes overlying these missed AF drivers were >2mm away from the tissue. In some instances, more organized reentrant arrhythmias, such as post-ablation atrial tachycardia (n=4, Online Figure 3) were also induced, and multi-electrode mapping consistently reproduced the macro-reentry pattern and location identified by NIOM.

Furthermore, FIRM could identify false-positive RAP outside NIOM-defined driver regions along with the RAP at true-positive drivers. Figure 5A shows correctly defined RAP at electrodes CD23 and EF23 overlying the two pivot points of the NIOM-defined reentrant AF driver (Figure 5B). Moreover, targeted ablation at EF23 successfully terminated AF, while the remaining 3 RAP locations were not involved in AF maintenance and represent false-positive RAP. In total, 18 false-positive RAP locations were identified (1.1±0.9 per AF visualization), 4 of which had one or more electrodes with no underlying atrial tissue, and therefore were excluded from NIOM analysis, just as false-positives identified at electrodes overhanging the atrioventricular annuli would be ignored by clinicians. In Figure 5B, NIOM activation maps show that false-positive RAP resulted from passive rotation, where activation rotates but does not make a self-sustaining circuit. Moreover, true-positive RAP locations had a NIOM-defined average and max PSD significantly higher than false-positive RAP locations (Figure 5C). There were no multi-electrode maps where false-positive RAP was marked without identifying at least one NIOM-defined AF driver in the same map (Online Table 3). False-positive RAP locations did not have a significantly lower FIRM DF or NIOM DF than AF drivers. Importantly, there was no significant difference in the

intensity of RAP between true-positive drivers and false-positives, which prevents FIRM alone from distinguishing them.

Fibrosis Architecture Distinguishes True-Positive from False-Positive RAP

High resolution (~100μm^3) CE-MRI shows the 3D distribution of intramural fibrosis in the lateral RA (Figure 6A) with histological analysis confirming the layers of epicardial and endocardial fibrosis as well as the specific intramural fibrosis insulated myobundles (Figure 6B). While the percentage of intramural fibrosis was significantly higher in NIOM-defined AF driver regions than in false-positive RAP and true-negative non-driver regions (Figure 6C), sub-epicardial, sub-endocardial, and total fibrosis values were not associated with true-positive AF drivers.

Discussion

Our study provides the first validation of clinically-visualized reentrant and focal patterns as AF drivers in human hearts. Our novel approach, integrating NIOM and 3D CE-MRI with clinical multi-electrode mapping, demonstrates that both stable or repetitive reentrant and focal surface visualizations of AF drivers may stem from intramural microanatomic reentry and could represent targets for ablation treatment. False-positive “drivers” could also be visualized by clinical multi-electrode mapping because of passively rotating fibrillatory waves or phase processing of electrograms with poor signal quality. Furthermore, by defining structural and electrophysiologic fingerprints of human AF drivers, our results emphasize that further integration of clinical multi-electrode mapping with intramural 3D fibrosis distribution may help differentiate true-positive AF drivers from false-positives, which could improve the success of driver targeted ablation.

Validation of Clinically Visualized AF Drivers

FIRM mapping of AF drivers matched surface visualization pattern and location seen by NIOM in only 70% and 80% of cases, respectively. These discrepancies in driver visualization may be due to differences in the nature of signal collection. NIOM collects signals at high resolution (up to 0.3mm^2) and uses near-infrared voltage sensitive dyes to record optical transmembrane action potentials over a depth of 4mm, and does not rely on contact with the tissue.(15) On the other hand, conventional unipolar and bipolar multi-electrode mapping have relatively low resolution and rely on direct contact with the tissue to detect extracellular potentials, which may be contaminated by far-field signals.(19,20) Thus, a reentry circuit could be misinterpreted as a focal pattern (Figure 4, Online Figure 4) or completely missed, due to low resolution of panoramic electrode mapping (~9mm^2 for FIRM). Even the highest resolution (5.6-7mm) panoramic biatrial epicardial clinical multi-electrode mapping study to date by the Waldo group(21) visualized predominantly focal/breakthrough patterns rather than reentry. However, current clinical high-resolution multi-electrode arrays (2-2.5mm^2)(8,22) have only small tissue coverage; thus, the lack of a stable driver signal in these studies may result from missing the driver entirely.

Additionally, two of the four AF drivers that were missed by FIRM were due to poor tissue contact in driver regions. Clinically, the spherical shape of the basket catheter used for

mapping may not make good tissue contact with the non-spheroidal atrial chambers. We recently reviewed(23) the challenge of ensuring good contact across the human atria wall which varies from 0.1 to 12mm thick(17). Dual-sided multi-electrode arrays(8) may have direct contact only with the thickest pectinate bundles; thus, driving reentry along small, intramural bundles could be visualized at the surface as breakthrough or mistaken entirely as multiwavelets.

A recent clinical study by de Groot and colleagues(8) used local dual-sided multi-electrode arrays, inserted from an incision in the right atrial appendage to map activation patterns in 14 patients with and without AF. Their analysis of AF patterns demonstrated dissociation of endo-epicardial activation and focal waves/breakthroughs in all patients, but they did not report reentrant activity. Although this contact multi-electrode study would suffer from the same obstacles facing FIRM contact electrodes, the discrepancies in driver identification may stem from factors other than those listed above. First, the high-resolution dual-sided array only covers a 14×30mm section of the right atrium versus the panoramic FIRM, and waves entering from the periphery of the array were not eligible for their driver definition. Second, the de Groot et al study(8) placed restrictions on what were considered continuous waves by activation time delays between electrodes while FIRM has no such restrictions. Third, other factors that varied between the two approaches but have unknown effects on driver detection are electrode sizes, interpolation, and filtering in electrograms, as we recently reviewed.(10) However, only the direct recording of FIRM-defined AF drivers by the dual-sided multi-electrode array used in the de Groot et al study(8) in the same heart, or validation of the dual-sided array by optical mapping ex-vivo, could reconcile the differences in AF patterns revealed between these techniques.

Early ex-vivo animal studies found that differences between optical and electrogram activation times stemmed primarily from the increased depth of interrogation by optical mapping.(20,24) Our recent dual-sided NIOM study of the human atria showed epi-endocardial dissociation up to 105ms during AF.(15) Moreover, atrial wall thickness variation, myofiber orientation misalignment, and intramural fibrosis(8,15) could lead to asynchronous activation of the partially discontinuous neighboring myocardial layers, thereby causing activation discordance and fractionation on a bipolar electrogram.(15,23) Nevertheless, clinical studies using both FIRM(5) and CARTOFINDER(25) found spatially stable AF drivers, which could be visualized with both focal and reentrant patterns; likewise, the microanatomic reentrant AF drivers observed in our ex-vivo studies were visualized by FIRM with similar patterns, which suggests that the mechanism of AF maintenance could be similar in in-vivo and ex-vivo human atria.

Our study observed AF drivers in both the right and left atrium. Ever since the pulmonary veins were shown to be sources of triggers in the initiation of AF, AF treatment has focused mainly on left atrial ablation. However, recent panoramic atrial mapping studies, which have found AF drivers using a variety of techniques, observed drivers in both the left and right atria.(4,5,21) The data suggests that patients with more persistent forms of AF may have more right atrial drivers than those with paroxysmal AF, which suggests that patient-specific AF drivers could be more efficient targets in the persistent AF population rather than pulmonary triggers.(5)

Pros and Cons of Phase Mapping to Identify Reentrant AF Drivers

To bypass the challenge of marking activation times during AF,(13,14) instantaneous phase analysis has been applied to identify PS or the center of rotational activity in clinical AF mapping. This is the first study that identifies intramural reentrant AF drivers by phase analysis of high-resolution NIOM in the ex-vivo human heart. Since the highest PSD clusters were found at reentrant AF driver sites, our study supports the cautious use of phase processing of multielectrode mapping in AF patients.

Noticeably, PSs seen clinically are suggested to represent the functional core of “rotors” capable of meandering across the atrium,(3,26) which raises concerns regarding targeted ablation of “rotor”-driven AF.(27) However, clinical multi-electrode mapping is unable to distinguish between microanatomic reentries, rotors, or focal AF drivers. Indeed, our study observed that FIRM could visualize NIOM reentry as focal activity (Figure 4, Online Figure 4). Furthermore, our data also suggest that clinically visualized drifting/meandering “rotors” could be a misinterpretation by phase processing of an elongated microanatomic reentry track formed by partially discontinuous myobundles. Our findings are supported by clinical ECGI studies that also observed intermittent yet recurring PS in driver regions.(4) The recent 64-electrode basket catheter mapping study(25) processed with CARTOFINDER activation mapping of unipolar electrograms, also identified ablatable localized drivers in almost all patients in the form of intermittent but repetitive focal or rotational activation patterns.

Our findings could also explain the lack of temporal stability or intermittency of AF drivers, a critical limitation of clinical recordings. First, as we described above, surface activation does not always portray intramural activation. Thus, surface visualization of microanatomic 3D reentrant drivers may be obscured as beat-to-beat fibrillatory conduction changes around the continuously active driver. Secondly, PS temporal stability at microanatomic reentrant drivers may also be intermittent or interrupted due to the elongated structure of the reentrant track and not the existence of a functional “rotor” (Online Figure 2). Lastly, if more than one driver was identified (Figure 3), each may not be continuously present and may instead disappear and reoccur at the same atrial region; however, at least one driver was always active during sustained AF.(16)

Even though phase-based mapping may provide an opportunity to visualize reentrant AF drivers in the clinical setting, it is also biased toward rotational visualization, which may lead to false-positive RAP identification(11,14,28) as observed in our study. False-positive targets might explain some of the discrepancies between clinical studies using FIRM(3,5,6). Thus, exclusion criteria identified by ex-vivo studies might provide a valuable approach to accurately distinguish between true-positive and false-positive RAP.

Interestingly, there were no apparent differences between true-positive drivers and false-positive RAP by either RAP intensity or NIOM and FIRM DF. However, we found that false-positive RAP locations were defined by lower max NIOM PSD than drivers. While RAP is partly based on PSD analysis(13) further studies are required to understand how differences between these two methods, such as resolution, may affect AF driver identification.

One possible explanation for the clinically visualized false-positive “drivers” may be fibrillatory conduction block causing repetitive passive rotation (Figure 5). Rudy and colleagues(11) recently reported that phase processing can create PSs at regions of conduction block, which do not represent self-sustaining reentrant activity and instead could be mistaken as false-positive “rotors”.(14,28) Our results also revealed that false-positive RAP could form at structural/functional conduction blocks (Figure 5) with less intramural fibrosis than NIOM-confirmed driver regions (Figure 6). These important findings suggest that mapping intramural atrial fibrosis may be particularly useful in identifying AF drivers.

Intramural Fibrosis as a Distinguishing “Fingerprint” of Reentrant AF Drivers

Clinical and experimental studies have shown that increased fibrosis is a significant contributor to the dysfunctional effects of atrial remodeling.(9,23,29) Our current study suggests that AF drivers can be distinguished from non-driver areas by the extent of intramural fibrosis. Furthermore, we could eliminate 5/14 false-positive RAP if a threshold of >12% intramural fibrosis by ex-vivo CE-MRI (Figure 6) is applied for a RAP region to qualify as an AF driver region in our data set. Our recent experimental(15,17) and computational studies from other groups(30) suggest that fibrotic architecture in the border zones of dense fibrosis may be more arrhythmogenic than the dense patch. Moreover, our human atria studies (17,23)also suggested that only fibrosis affecting the path of conduction could be arrhythmogenic, in contrast to fibrosis that naturally covers the epicardial or endocardial surfaces (Figure 6). Based on our recent(17) and current data (Figure 6), we suggest that arrhythmogenic intramural fibrosis may be considered a unique fingerprint of intramural reentrant AF drivers..

However, assessing the 3D architecture of intramural fibrosis in human atria may prove difficult for clinical MRI. Although our CE-MRI methodology mimics that used clinically(29) with resolution 1.25mm^3, the higher magnet strength allowed us to acquire the considerably higher resolution of ~0.1mm^3 in the ex-vivo human atria. As such, the right atrial wall with an average thickness of ~4mm can contain ~22 voxels even at the lowest resolution done in our study (~0.180mm3), which successfully allowed us to differentiate between sub-endocardial, sub-epicardial and intramural fibrosis (Figure 6). Conflicting results have been reported from clinical studies that have looked for a correlation between late gadolinium enhanced MRI (LGE-MRI), a surrogate for fibrosis, and clinical AF driver locations. One study found that areas with high reentrant activity by ECGI showed higher local LGE-MRI density compared to other areas,(31) while no correlation between FIRM-defined AF drivers and LGE-MRI was found in another study.(32) These discrepancies could be explained by the limitation of clinical multi-electrode approaches as well as atrial LGE-MRI, which require further validation by ex-vivo CE-MRI and an increase in resolution to resolve 3D architecture of intramural fibrosis.

Recent clinical MRI(31) and postmortem histological(33) studies indicate that fibrosis can be similarly upregulated in both left and right atria in AF patients. Although several clinical multi-electrode mapping studies have shown that patients have not only left atrial drivers but often RA drivers as well,(4,21,34) it is currently unknown if RA drivers have similar or different structural substrates or fingerprints as left atrial drivers. This study and our

previous high-resolution CE-MRI study of the intact human atria(17) suggest that similar structural fingerprints might underlie drivers in both atria. However, rigorous studies directly comparing structural substrates of left and right atrial drivers are required to elucidate differences of clinical relevance.

Future Directions

It may be possible to bridge the gap between high-resolution NIOM and current clinical electrode mapping by complementing low-resolution panoramic catheters with high-resolution catheters. Furthermore, combining multiple analyses of electrode signals (i.e. phase, activation, and RAP) may provide stronger evidence of AF drivers.(13) Our data indicate that clinical multi-electrode mapping alone may lack the ability to distinguish true-positive drivers from false-positives. Thus, systematic clinical and experimental studies integrating 3D electrical and structural approaches are required to address the patient-specific 3D fibrotic architecture to better identify reentrant AF drivers for targeted ablation.

Limitations

Our study includes a small sample of ex-vivo human hearts with varied disease history; extrapolation of results to a wider AF population requires further in-vivo and ex-vivo studies. Due to the limited number of samples this study cannot definitively state what approach is superior for clinical AF mapping and ablation. We found no difference in fibrotic content between left and right atrial drivers; however, further studies are needed to uncover any subtle differences that may affect their identification or ablation. Our denervated and mechanically-arrested ex vivo atrial preparations are in the absence of both autonomic and metabolic stresses at baseline. Therefore, pharmacological autonomic (adenosine or isoproterenol)(16) or metabolic (pinacidil) stimulations(15) were used to include autonomic and metabolic stresses known to play a critical role in AF and recapitulate clinical conduction and repolarization.(9) For the direct comparison of NIOM and FIRM, clinical FIRMap basket catheters were flattened, however, electrode size and data analysis remained the same.

Conclusions

This study provides the first validation and mechanistic explanation of localized reentrant and/or focal human AF drivers as visualized by clinical multi-electrode mapping and identifies conditions when drivers may potentially be misinterpreted. Integrated electrophysiological and structural mapping can identify unique structural fingerprints of AF drivers to distinguish true-positive from false-positive AF drivers, but warrants further validation in the clinical setting. If validated in patients, our findings could lead to a more comprehensive and precise understanding of the fundamental mechanisms of AF in patients and improve the success rate of driver targeted catheter ablation and minimizing the amount of tissue damage.

Supplementary Material

Refer to Web version on PubMed Central for supplementary material.

Acknowledgments:

We thank the Lifeline of Ohio Organ Procurement Organization and the Division of Cardiac Surgery at The OSU Wexner Medical Center for providing the explanted hearts. The human heart repository program is supported by the Davis Heart and Lung Research Institute. We thank Ms. Esthela Artiga for critical reading of the manuscript. We also thank Abbott engineers Mr. Brian Pederson and Mr. Carey Briggs, for their help in integrating FIRM mapping and data analysis of FIRM recordings.

Sources of Funding: This work was supported by NIH HL115580 and HL135109, and American Heart Association Grant in Aid #16GRNT31010036 (VVF), Health Research Council of New Zealand (JZ) and NIH T32HL134616 (BJH).

Disclosures: Dr. Fedorov has received research support from Abbott Laboratories. Dr. Hummel is a Consultant to Abbott Laboratories. Dr. Simonetti receives research support from Siemens.

Abbreviations

AF	Atrial Fibrillation
RA	Right Atrium
LA	Left Atrium
FIRM	Focal Impulse and Rotor Mapping
ECGI	Electrocardiographic Imaging
PS(D)	Phase Singularity (Density)
RAP	Rotational Activity Profile
NIOM	Near-infrared Optical Mapping
CE-MRI	Contrast-enhanced Magnetic Resonance Imaging
LGE-MRI	Late Gadolinium-Enhanced Magnetic Resonance Imaging

Reference List

1. Chugh SS, Havmoeller R, Narayanan K et al. Worldwide epidemiology of atrial fibrillation: a Global Burden of Disease 2010 Study. Circulation 2014;129(8):837–847. [PubMed: 24345399]
2. Calkins H, Hindricks G, Cappato R et al. 2017 HRS/EHRA/ECAS/APHRS/SOLAECE expert consensus statement on catheter and surgical ablation of atrial fibrillation. Europace 2018;20(1):e1–e160.
3. Narayan SM, Krummen DE, Shivkumar K et al. Treatment of atrial fibrillation by the ablation of localized sources: CONFIRM (Conventional Ablation for Atrial Fibrillation With or Without Focal Impulse and Rotor Modulation) trial. J Am Coll Cardiol 2012;60(7):628–636. [PubMed: 22818076]
4. Haissaguerre M, Hocini M, Denis A et al. Driver domains in persistent atrial fibrillation. Circulation 2014;130(7):530–538. [PubMed: 25028391]
5. Miller JM, Kalra V, Das MK et al. Clinical Benefit of Ablating Localized Sources for Human Atrial Fibrillation: The Indiana University FIRM Registry. J Am Coll Cardiol 2017;69(10):1247–1256. [PubMed: 28279291]
6. Benharash P, Buch E, Frank P et al. Quantitative Analysis of Localized Sources Identified by Focal Impulse and Rotor Modulation Mapping in Atrial Fibrillation. Circ Arrhythm Electrophysiol 2015;8(3):554–561. [PubMed: 25873718]

7. Jalife J, Filgueiras RD, Berenfeld O. Letter by Jalife et al. Regarding Article, "Quantitative Analysis of Localized Sources Identified by Focal Impulse and Rotor Modulation Mapping in Atrial Fibrillation". Circ Arrhythm Electrophysiol 2015;8(5):1296–1298. [PubMed: 26487627]
8. de Groot N, van der Does L, Yaksh A et al. Direct Proof of Endo-Epicardial Asynchrony of the Atrial Wall During Atrial Fibrillation in Humans. Circ Arrhythm Electrophysiol 2016;9(5):e003648. [PubMed: 27103089]
9. Heijman J, Guichard JB, Dobrev D, Nattel S. Translational Challenges in Atrial Fibrillation. Circ Res 2018;122(5):752–773. [PubMed: 29496798]
10. Hansen BJ, Csepe TA, Zhao J et al. Maintenance of Atrial Fibrillation: Are Reentrant Drivers With Spatial Stability the Key? Circ Arrhythm Electrophysiol 2016;9(10):e004398. [PubMed: 27729340]
11. Vijayakumar R, Vasireddi SK, Cuculich PS, Faddis MN, Rudy Y. Methodology Considerations in Phase Mapping of Human Cardiac Arrhythmias. Circ Arrhythm Electrophysiol 2016;9(11): e004409. [PubMed: 27906655]
12. Sahli Costabal F, Zaman JAB, Kuhl E, Narayan SM. Interpreting Activation Mapping of Atrial Fibrillation: A Hybrid Computational/Physiological Study. Ann Biomed Eng 2018;46(2):257–269. [PubMed: 29214421]
13. Alhusseini M, Vidmar D, Meckler GL et al. Two Independent Mapping Techniques Identify Rotational Activity Patterns at Sites of Local Termination During Persistent Atrial Fibrillation. J Cardiovasc Electrophysiol 2017;28(6):615–622. [PubMed: 28185348]
14. Rodrigo M, Climent AM, Liberos A et al. Technical Considerations on Phase Mapping for Identification of Atrial Reentrant Activity in Direct- and Inverse-Computed Electrograms. Circ Arrhythm Electrophysiol 2017;10(9):e005008. [PubMed: 28887361]
15. Hansen BJ, Zhao J, Csepe TA et al. Atrial fibrillation driven by micro-anatomic intramural re-entry revealed by simultaneous sub-epicardial and sub-endocardial optical mapping in explanted human hearts. Eur Heart J 2015;36(35):2390–2401. [PubMed: 26059724]
16. Li N, Csepe TA, Hansen BJ et al. Adenosine-Induced Atrial Fibrillation: Localized Reentrant Drivers in Lateral Right Atria due to Heterogeneous Expression of Adenosine A1 Receptors and GIRK4 Subunits in the Human Heart. Circulation 2016;134(6):486–498. [PubMed: 27462069]
17. Zhao J, Hansen BJ, Wang Y et al. 3D Integrated functional, structural, and computational mapping to define the structural "fingerprints" of heart-specific atrial fibrillation drivers in human heart ex-vivo . J Am Heart Assoc 2017;6(8):e005922. [PubMed: 28862969]
18. Gray RA, Pertsov AM, Jalife J. Spatial and temporal organization during cardiac fibrillation. Nature 1998;392:75–78. [PubMed: 9510249]
19. van der Does LJ, de Groot NM. Inhomogeneity and complexity in defining fractionated electrograms. Heart Rhythm 2017;14(4):616–624. [PubMed: 28104483]
20. Walton RD, Smith RM, Mitrea BG et al. Extracting surface activation time from the optically recorded action potential in three-dimensional myocardium. Biophys J 2012;102(1):30–38. [PubMed: 22225795]
21. Lee S, Sahadevan J, Khrestian CM et al. Simultaneous Biatrial High-Density (510-512 Electrodes) Epicardial Mapping of Persistent and Long-Standing Persistent Atrial Fibrillation in Patients: New Insights Into the Mechanism of Its Maintenance. Circulation 2015; 132(22):2108–2117. [PubMed: 26499963]
22. Lee G, Kumar S, Teh A et al. Epicardial wave mapping in human long-lasting persistent atrial fibrillation: transient rotational circuits, complex wavefronts, and disorganized activity. Eur Heart J 2014;35(2):86–97. [PubMed: 23935092]
23. Hansen BJ, Zhao J, Fedorov VV. Fibrosis and Atrial Fibrillation: Computerized and Optical Mapping: A View Into the Human Atria at Submillimeter Resolution. J Am Coll Cardiol EP 2017;3(6):531–546.
24. Himel HD, Knisley SB. Comparison of optical and electrical mapping of fibrillation. Physiol Meas 2007;28(6):707–719. [PubMed: 17664624]
25. Honarbakhsh S, Schilling RJ, Dhillon G et al. A Novel Mapping System for Panoramic Mapping of the Left Atrium: Application to Detect and Characterize Localized Sources Maintaining Atrial Fibrillation. JACC Clin Electrophysiol 2018;4(1):124–134. [PubMed: 29387810]

26. Berenfeld O, Jalife J. Mechanisms of atrial fibrillation: rotors, ionic determinants, and excitation frequency. Cardiol Clin 2014;32(4):495–506. [PubMed: 25443232]
27. Weiss JN, Qu Z, Shivkumar K. Ablating atrial fibrillation: A translational science perspective for clinicians. Heart Rhythm 2016;13(9):1868–1877. [PubMed: 27241354]
28. Kuklik P, Zeemering S, van HA et al. Identification of Rotors during Human Atrial Fibrillation Using Contact Mapping and Phase Singularity Detection: Technical Considerations. IEEE Trans Biomed Eng 2017;64(2):310–318. [PubMed: 27101596]
29. Marrouche NF, Wilber D, Hindricks G et al. Association of atrial tissue fibrosis identified by delayed enhancement MRI and atrial fibrillation catheter ablation: the DECAAF study. JAMA 2014;311(5):498–506. [PubMed: 24496537]
30. Zahid S, Cochet H, Boyle PM et al. Patient-derived models link re-entrant driver localization in atrial fibrillation to fibrosis spatial pattern. Cardiovasc Res 2016;110(3):443–454. [PubMed: 27056895]
31. Cochet H, Dubois R, Yamashita S et al. Relationship between Fibrosis detected on Late Gadolinium-enhanced MRI and Reentrant Activity assessed with ECGI in Human Persistent Atrial Fibrillation. J Am Coll Cardiol EP 2018;4(1):17–29.
32. Chrispin J, Gucuk IE, Zahid S et al. Lack of regional association between atrial late gadolinium enhancement on cardiac magnetic resonance and atrial fibrillation rotors. Heart Rhythm 2016;13(3):654–660. [PubMed: 26569460]
33. Platonov PG, Mitrofanova LB, Orshanskaya V, Ho SY. Structural abnormalities in atrial walls are associated with presence and persistency of atrial fibrillation but not with age. J Am Coll Cardiol 2011;58(21):2225–2232. [PubMed: 22078429]
34. Friedman DJ, Liu P, Barnett AS et al. Obstructive sleep apnea is associated with increased rotor burden in patients undergoing focal impulse and rotor modification guided atrial fibrillation ablation. Europace 2017;doi: 10.1093/europace/eux248.

Clinical Perspectives

Competency in Patient Care and Procedural Skills:

While clinical multi-electrode mapping may successfully detect localized reentrant AF drivers, it also has the propensity to detect false positive reentrant patterns; hence, caution should be taken to prevent unnecessary ablation in AF patients.

Competency in Medical Knowledge:

Clinical multi-electrode mapping at the atrial surfaces can visualize intramural microanatomic reentrant AF drivers in the human heart as both reentrant and focal activation patterns, which represent viable targets for efficient ablation treatment.

Translational Outlook:

AF drivers could be predominantly located in regions of the atria with more intramural fibrosis than in regions with false-positive reentrant patterns. Further clinical studies are required to assess the benefits of integrating 3D structural imaging with multi-electrode mapping for designing successful AF driver targeted ablation treatments.

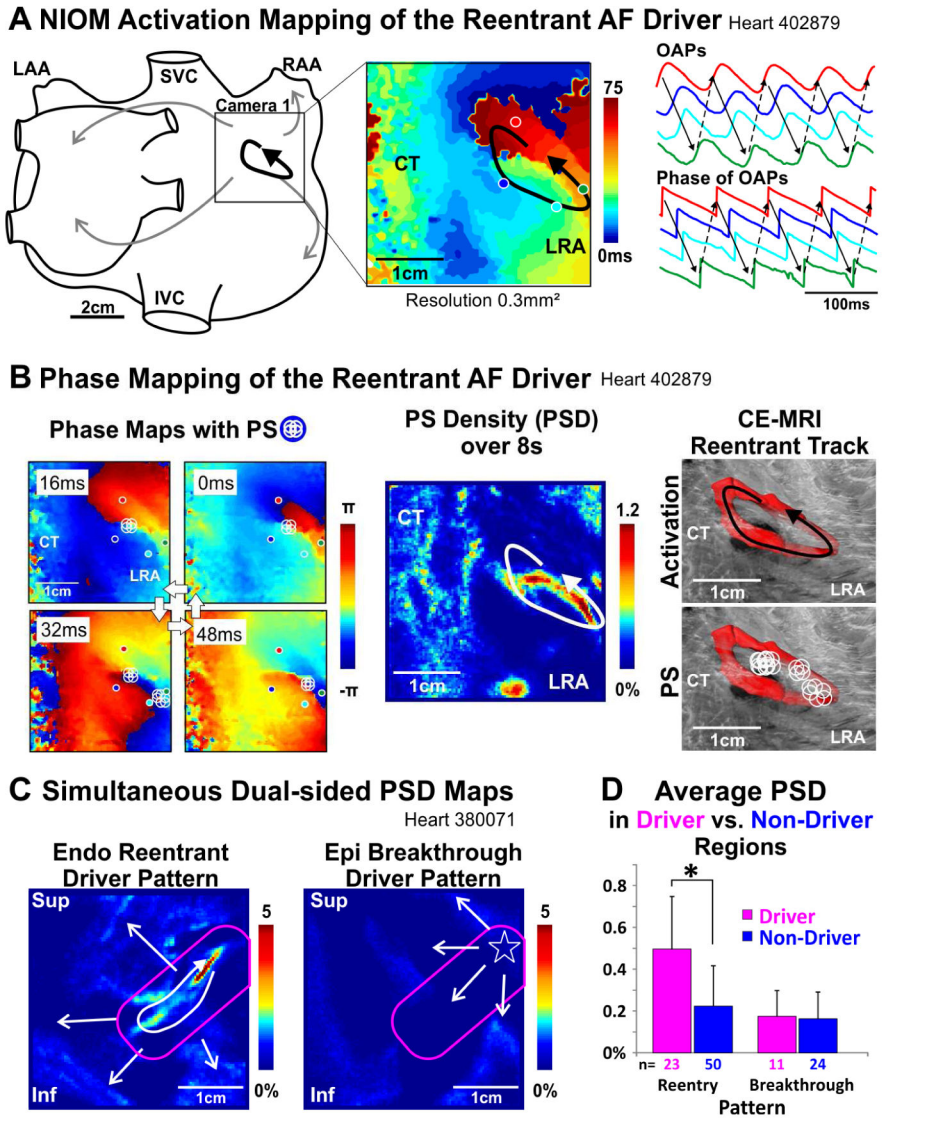

Figure 1. AF Driver Identification by NIOM Activation and Phase Mapping.

A. NIOM activation map, optical action potentials (OAPs), and their phase of a reentrant AF driver. B. Left to Right, snapshots of instantaneous phase maps with phase singularities (PS) shown by white circles; Phase singularity density (PSD) map; 3D contrast-enhanced MRI (CE-MRI) reconstruction of the reentrant track in red with overlaid reentrant activity and PSs. C. Simultaneous dual-sided PSD maps of reentrant and breakthrough patterns. Driver regions outlined in pink. D. Average PSD in driver vs non-driver regions. *P<0.05. AF-atrial fibrillation; CT-crista terminalis; Endo-endocardium; Epi-epicardium; NIOM-near infrared optical mapping; Inf/Sup-inferior/superior lateral right atrium (LRA); IVC/SVC-inferior/superior vena cava; LAA/RAA-left/right atrial appendage.

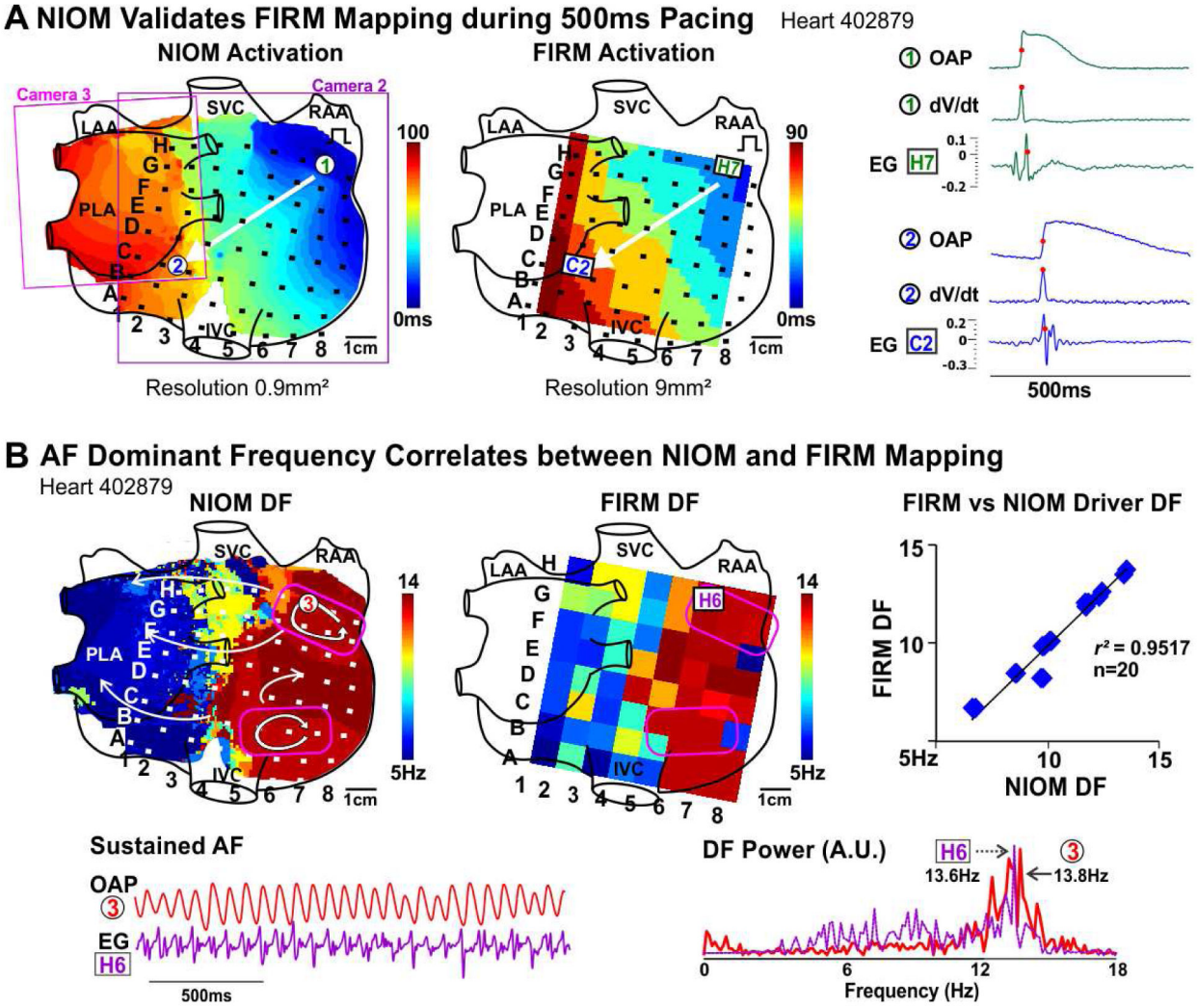

Figure 2. Correlation between NIOM and Focal Impulse and Rotor Mapping (FIRM) Activation Patterns and AF Dominant Frequency.

A. Activation maps from NIOM (Left) and FIRM (Middle) during 500ms pacing. FIRM electrodes shown as black squares. Right, OAPs, their derivatives (dV/dt), and neighboring electrograms. Activation times marked by red dots. B. NIOM dominant frequency (DF, Left) and FIRM DF (Middle) maps. Right, average correlation between NIOM and FIRM DF. Driver regions outlined in pink. OAP, EG, their DF spectrum shown below. Abbreviations as in Figure 1; PLA-posterior left atrium, EG-electrogram.

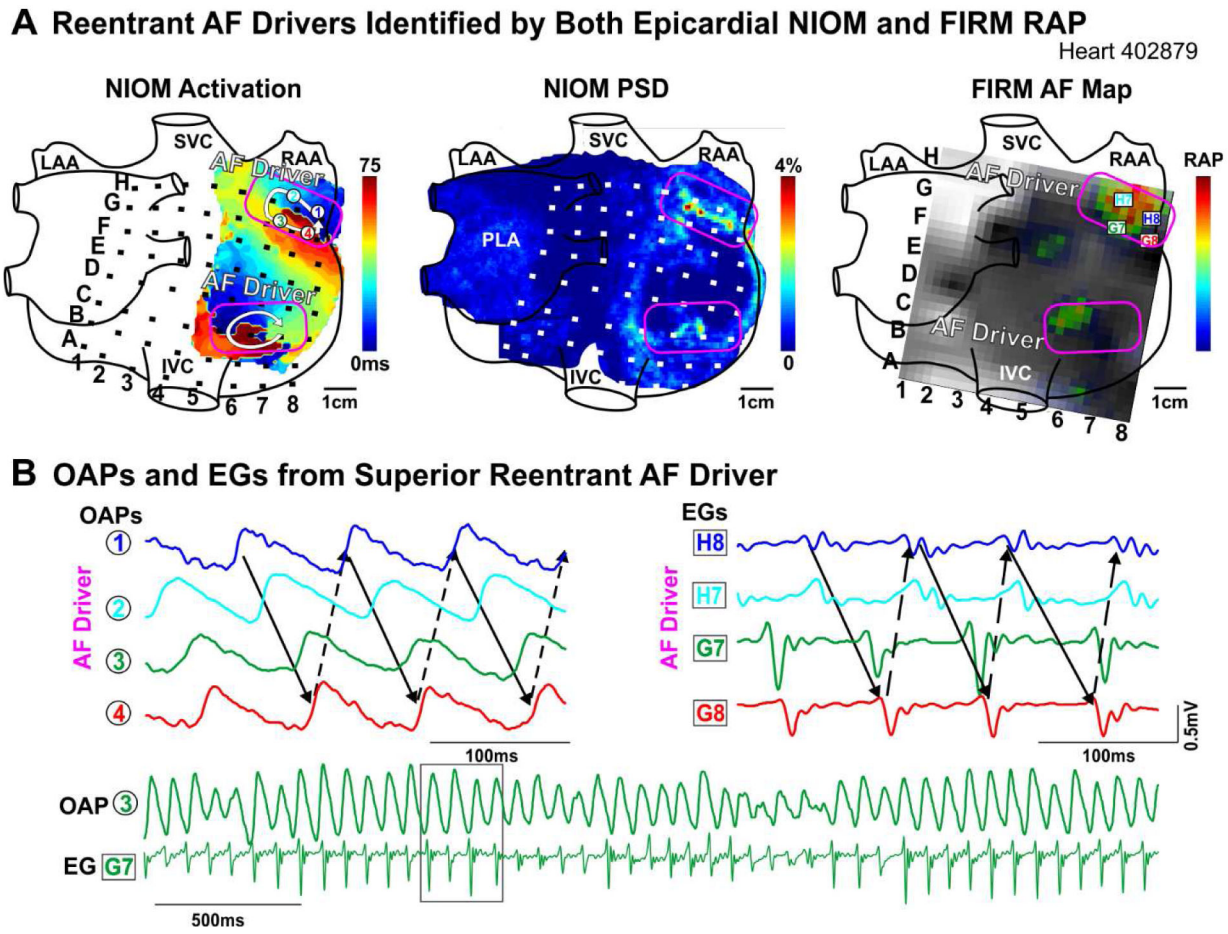

Figure 3. Reentrant AF Drivers Visualized by NIOM and FIRM.

A. Left to Right: Epicardial NIOM activation map; NIOM PSD map; and snapshot of epicardial FIRM movie with rotational activity profiles (RAP). NIOM-defined drivers outlined in pink. B. OAPs and unipolar FIRM EGs, black box shows time window for OAPs and EGs above. Abbreviations as in Figure 2.

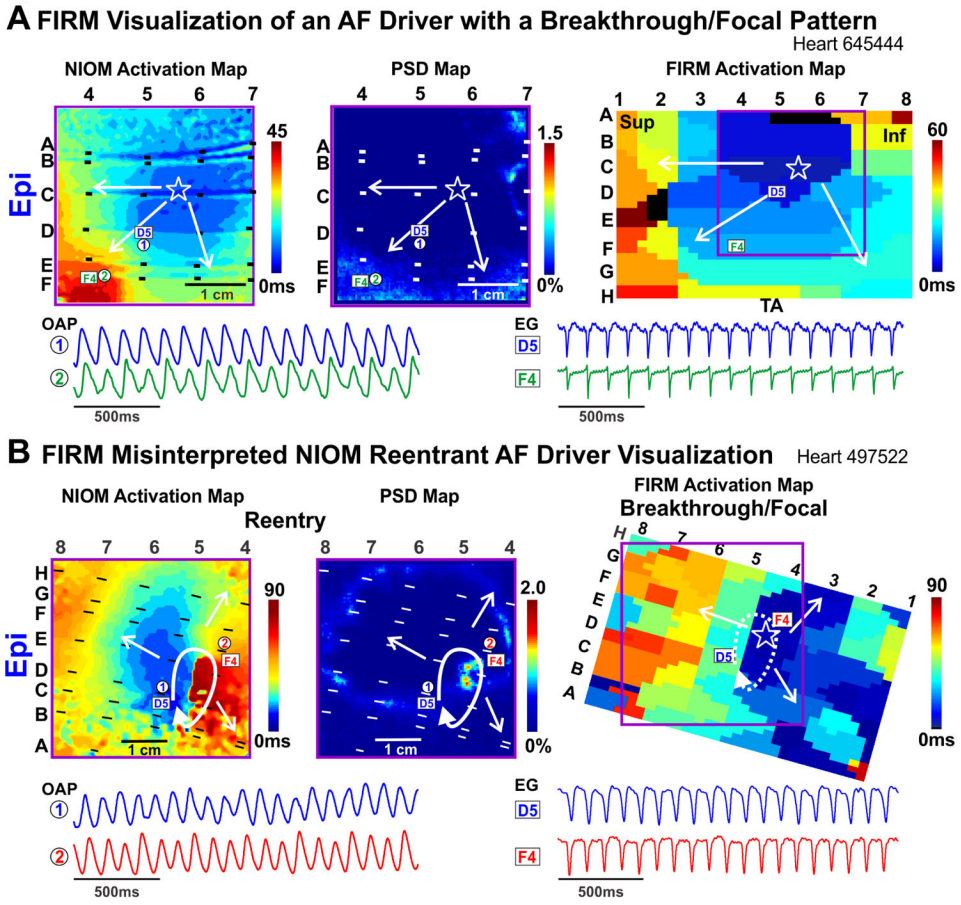

Figure 4. Focal Activation Pattern Seen by FIRM Overlies Both Breakthrough and Reentrant Driver Patterns.

A. NIOM activation (Left), NIOM PSD (Middle), and FIRM activation (Right) maps of an AF driver recorded from the epicardial surface as a breakthrough/focal pattern (star). OAPs and EGs shown below. B. NIOM activation (Left), NIOM PSD (Middle), and FIRM activation (Right) maps of a reentrant AF driver seen as breakthrough/focal pattern by FIRM from the epicardial surface. OAPs and EGs shown below. Abbreviations as in Figure 2; TA-tricuspid annulus.

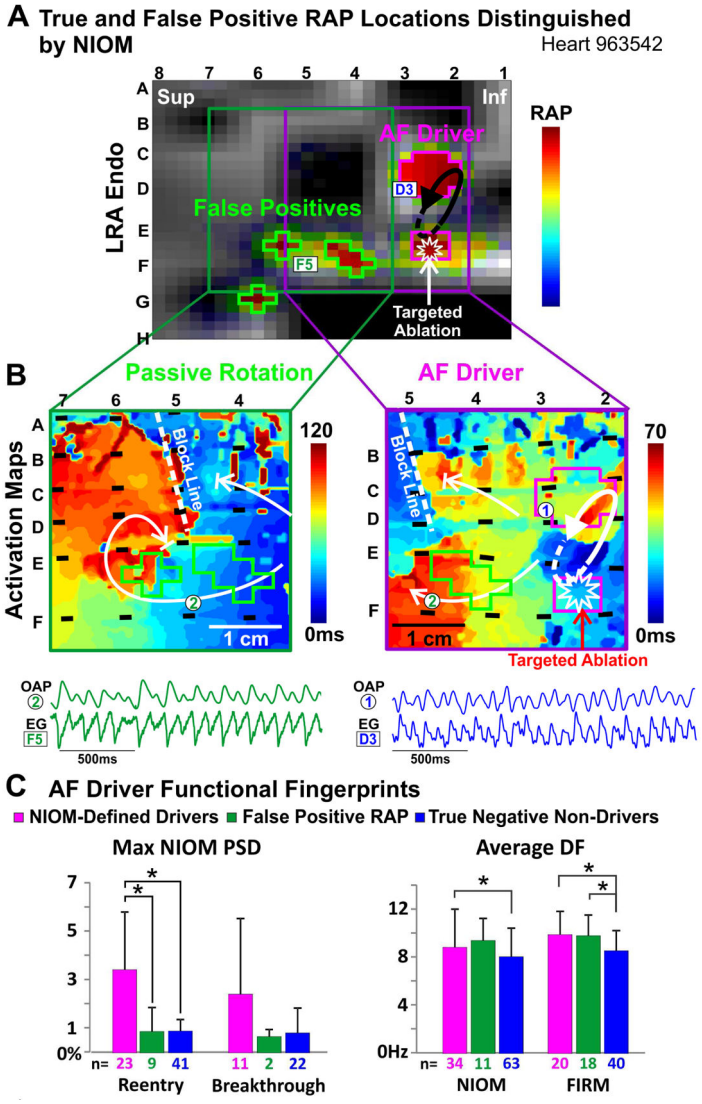

Figure 5. True-Positive and False-Positive AF Drivers Seen by FIRM.

A. Snapshot of FIRM movie with both false-positive and true-positive RAP locations, outlined in green and pink, respectively. EGs shown below. B. NIOM activation maps showing passive rotation at false positive RAP locations in green (Left) and a reentrant AF driver at the RAP locations in pink (Right). C. Max PSD and Average DF in NIOM-defined driver, false-positive RAP, and true-negative non-driver regions. *P<0.05. Abbreviations as in Figure 4.

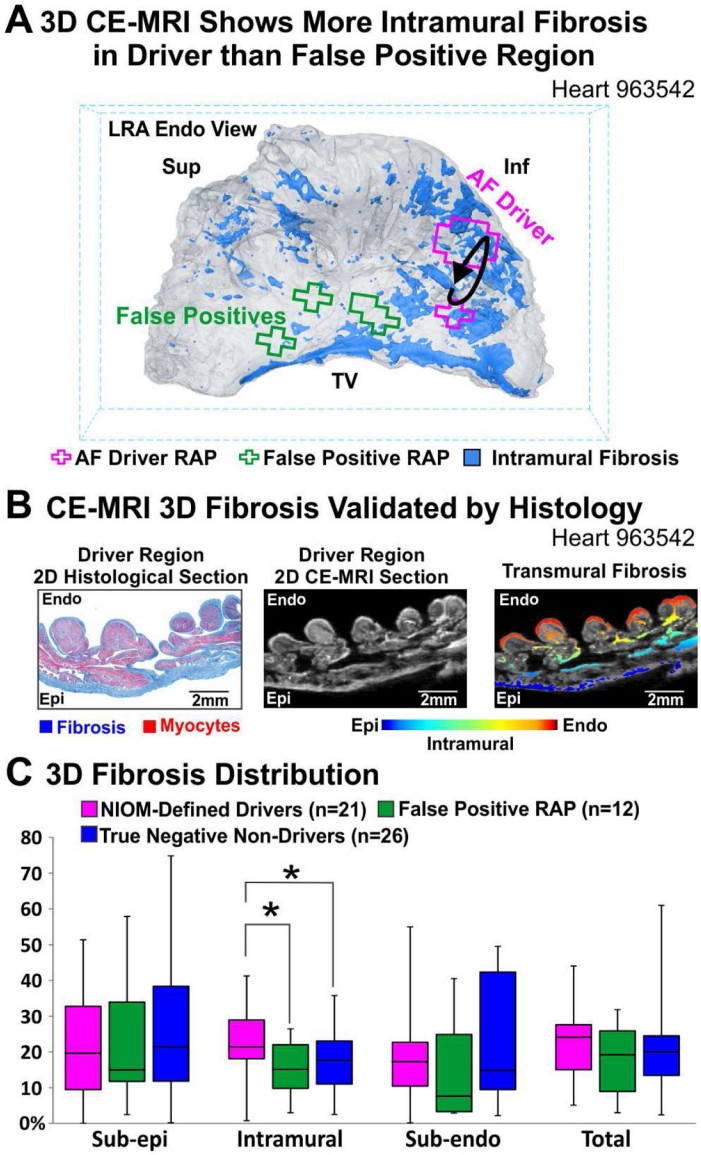

Figure 6. 3D Distribution of Fibrosis in AF Driver vs False Positive Regions.

A. 3D CE-MRI of LRA showing that higher intramural fibrosis (blue) underlies AF driver RAP regions (pink) than false positive RAP regions (green). B. 2D transmural sections from the driver region (Left to Right) with Masson's Trichrome staining, show fibrosis in blue; CE-MRI fibrosis in white; CE-MRI with fibrosis color-coded for transmural location. C. Percent of fibrotic tissue by transmural location. *P<0.05. Abbreviations as in Figure 4; TV-tricuspid valve.

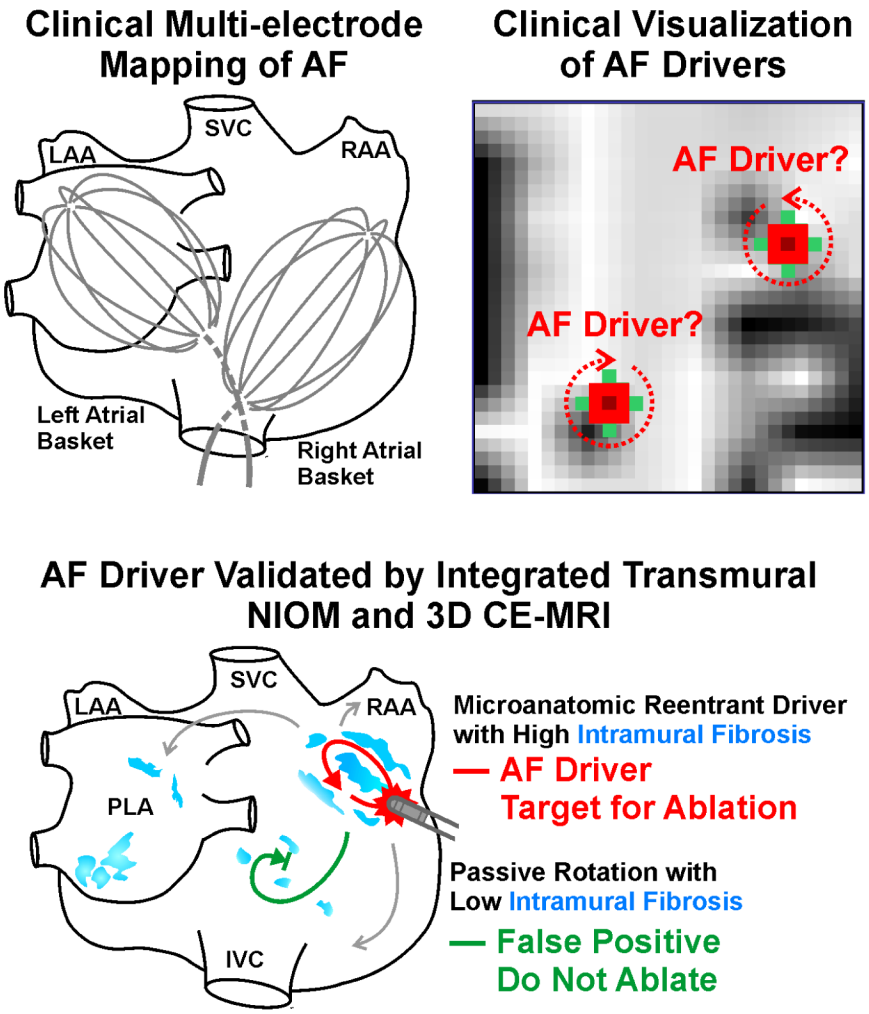

Central Illustration. Clinical Multi-electrode Mapping of AF drivers Validated by 3D Functional and Structural Mapping.

Top Left to Right, Clinical multi-electrode catheters mapping AF in the human atria and clinical visualization of reentrant AF drivers. Bottom, AF driver validated by integrated NIOM and 3D CE-MRI and distinguished from false-positive. A reentrant driver within a region of high intramural fibrosis would be a viable target for ablation, and false-positive passive rotation within a region of low intramural fibrosis should not be ablated. AF-atrial fibrillation; CE-MRI-contrast enhanced MRI; NIOM-near infrared optical mapping.